Seasonal blooms of neutrophilic Betaproteobacterial Fe(II) oxidizers and Chlorobi in iron-rich coal mine drainage sediments

Blackwell, Nia Lyn; Perkins, Bill; Palumbo-Roe, Barbara; Bearcock, Jenny M.; Lloyd, Jonathan R.; Edwards, Arwyn

Published in:
FEMS Microbiology Ecology

DOI:
10.1093/femsec/fiz140

Publication date:
2019

Citation for published version (APA):
Blackwell, N. L., Perkins, B., Palumbo-Roe, B., Bearcock, J. M., Lloyd, J. R., & Edwards, A. (2019). Seasonal blooms of neutrophilic Betaproteobacterial Fe(II) oxidizers and Chlorobi in iron-rich coal mine drainage sediments. *FEMS Microbiology Ecology*, *95*(10), [fiz140]. https://doi.org/10.1093/femsec/fiz140

FEMS Microbiology Ecology, 95, 2019, fiz140

doi: 10.1093/femsec/fiz140
Advance Access Publication Date: 5 September 2019
Research Article

RESEARCH ARTICLE

Seasonal blooms of neutrophilic *Betaproteobacterial* Fe(II) oxidizers and *Chlorobi* in iron-rich coal mine drainage sediments

Nia Blackwell[1,*,†,‡], William Perkins[1], Barbara Palumbo-Roe[2], Jenny Bearcock[2], Jonathan R. Lloyd[3] and Arwyn Edwards[1,4]

[1]Department of Geography and Earth Sciences, Aberystwyth University, Aberystwyth, Ceredigion SY23 3DB, UK, [2]British Geological Survey, Environmental Science Centre, Nicker Hill, Keyworth, Nottingham NG12 5GG, UK, [3]Williamson Research Centre for Molecular Environmental Science, School of Earth, Atmospheric and Environmental Sciences, University of Manchester, Manchester, M13 9PL, UK and [4]Institute of Biological, Environmental and Rural Sciences (and Interdisciplinary Centre for Environmental Microbiology, and Centre for Glaciology), Aberystwyth University, Aberystwyth, SY23 3DA, UK

*Corresponding author: Center for Applied Geosciences, 12 Hoelderinlinstrasse, 72070 Tuebingen, Germany; E-mail: nia.blackwell@uni-tuebingen.de

†Present address: Center for Applied Geosciences, 12 Hoelderlinstrasse, 72070 Tuebingen, Germany

One sentence summary: Microbial ecology of iron-rich sediments at an abandoned circumneutral coal mine drainage site in the South Wales Coalfield.

Editor: Tillmann Lueders

‡Nia Blackwell, http://orcid.org/0000-0002-6256-8449

ABSTRACT

Waters draining from flooded and abandoned coal mines in the South Wales Coalfield (SWC) are substantial sources of pollution to the environment characterized by circumneutral pH and elevated dissolved iron concentrations (>1 mg L^{-1}). The discharged Fe precipitates to form Fe(III) (oxyhydr)oxides which sustain microbial communities. However, while several studies have investigated the geochemistry of mine drainage in the SWC, less is known about the microbial ecology of the sites presenting a gap in our understanding of biogeochemical cycling and pollutant turnover. This study investigated the biogeochemistry of the Ynysarwed mine adit in the SWC. Samples were collected from nine locations within sediment at the mine entrance from the upper and lower layers three times over one year for geochemical and bacterial 16S rRNA gene sequence analysis. During winter, members of the *Betaproteobacteria* bloomed in relative abundance (>40%) including the microaerophilic Fe(II)-oxidizing genus *Gallionella*. A concomitant decrease in *Chlorobi*-associated bacteria occurred, although by summer the community composition resembled that observed in the previous autumn. Here, we provide the first insights into the microbial ecology and seasonal dynamics of bacterial communities of Fe(III)-rich deposits in the SWC and demonstrate that neutrophilic Fe(II)-oxidizing bacteria are important and dynamic members of these communities.

Keywords: neutrophilic Fe(II) oxidation; Fe(II)-oxidizing bacteria; coal mine drainage; ochreous sediments; spatiotemporal dynamics; mine drainage microbial ecology

Received: 27 March 2019; **Accepted:** 4 September 2019

INTRODUCTION

Iron is an abundant redox-active element that accounts for around 5% of the earth's crust (Faure 1998). The two main redox states in the environment are Fe(II) (ferrous iron) and Fe(III) (ferric iron) which play a crucial role in many environmental biogeochemical cycles including nitrogen, sulfur and carbon (Melton *et al.* 2014). There are numerous biotic and abiotic reactions in the Fe biogeochemical cycle that involve the oxidation of Fe(II) to Fe(III) to form Fe(III) (oxyhydr)oxide precipitates and the reduction of Fe(III) to Fe(II) (Melton *et al.* 2014). At circumneutral pH, Fe(II) is rapidly oxidized to Fe(III) by O_2 (Stumm and Morgan 1993) though this abiotic oxidation decreases substantially with decreasing O_2 concentrations, pH and temperature (Neubauer, Emerson and Megonigal 2002; Hedrich, Schlömann and Barrie Johnson 2011; Emerson *et al.* 2015). In the presence of reduced sulfur species such as H_2S, Fe(III) (oxyhydr)oxides are abiotically reduced (Canfield 1989; Yao and Millero 1996). Microbially mediated Fe(III) reduction involves reduction of Fe(III) by microorganisms that can use either H_2 or organic carbon as an electron donor (Lovley and Phillips 1988; Lovley 1997). At circumneutral pH, microorganisms capable of Fe(II) oxidation can be divided into three physiological groups: (i) anoxygenic nitrate-reducing, (Kappler, Schink and Newman 2005; Laufer *et al.* 2016c), (ii) anoxygenic phototrophic (Widdel *et al.* 1993) and (iii) microaerophilic (Emerson and Moyer 1997), the activities of which lead to the production of a variety of biogenic Fe(III) minerals (Bryce *et al.* 2018).

The occurrence of Fe(III) (oxyhydr)oxide minerals is widespread in many environments, at both acidic and circumneutral pH, which allows for the development of complex microbial communities with a range of metabolic activities that are capable of cycling Fe (Peine *et al.* 2000; Duckworth *et al.* 2009; Wang *et al.* 2009; Coby *et al.* 2011; Roden *et al.* 2012). More recent studies have focused on the temporal changes in microbial communities in Fe(III)-rich environments (Fabisch *et al.* 2013, 2016; Fleming *et al.* 2014). In environments where Fe cycling occurs, a vertically stratified microbial community may develop due to the formation of redox gradients (Duckworth *et al.* 2009). A theoretical framework for the distribution of Fe-cycling microbes based on the prevailing environmental conditions, thermodynamic and kinetic parameters, and the formation of geochemical niches has been proposed (Schmidt, Behrens and Kappler 2010). However, the distribution of Fe-cycling microbes can also be decoupled from geochemical gradients due to bioturbation, metabolic flexibility, the occurrence of microniches and habitats, or interrelationships with other microbial community members (Laufer *et al.* 2016b; Otte *et al.* 2018).

The temporal dynamics of Fe cycling affects the occurrence, abundance and persistence of reactive Fe(III) oxides in sediments (Roden 2012). This, in turn, affects the fate of other contaminants and metals, as Fe(III) (oxyhydr)oxide surfaces are known for their strong sorption capacity (Gadd 2004; Borch *et al.* 2010) and can affect the speciation and mobility of toxic contaminants (Vaughan and Lloyd 2011). Metals and contaminants associated with Fe(III) (oxyhydr)oxides (either incorporated into the structure or adsorbed to the surface) can be released during microbial reduction (Smedley and Kinniburgh 2002; Lloyd 2003; Rhine *et al.* 2005). Arsenic is a problematic metalloid in many lakes, rivers and aquifers and is detrimental to human health (Brammer and Ravenscroft 2009; Smedley and Kinniburgh 2013; Muehe and Kappler 2014). The role of Fe cycling in As mobilization has been a major focus of several studies and the activities of several bacteria have been shown to release As into the environment via Fe(III) mineral reductive mechanisms (Cummings *et al.* 1999; Islam *et al.* 2004). Conversely, Fe(II)-oxidizing bacteria can have a positive impact on the sequestration and removal of As from solution through the production of biogenic Fe(III) minerals. Numerous field and laboratory studies have shown the ability of Fe(III) (oxyhydr)oxides to act as sorbents for As (e.g. Dixit and Hering 2003; Hohmann *et al.* 2010; Keim 2011), especially in circumneutral environments (Sowers *et al.* 2017). Therefore, identifying Fe-cycling microbial communities present in contaminated environments, such as abandoned mines, is imperative. Furthermore, understanding the temporal changes in microbial communities associated with Fe(III)-rich environments is critical and has wider implications on contaminant dynamics.

The South Wales Coalfield (SWC), UK, has a long history of mining activity, mainly for the high-grade anthracitic coal. However, some of the worked coal seams contain elevated concentrations of pyrite and arsenopyrite (2–4% pyritic S) (Evans, Watkins and Banwart 2006), and consequently the discharge from many of the abandoned mines is contaminated with Fe and, occasionally, As (Sapsford *et al.* 2015). The pH of these mine waters is typically circumneutral due to the buffering capacity of the underlying geology and, as such, Fe(III)-rich ochreous deposits are widespread within the SWC. In recent years, there have been several studies investigating the geochemistry of these mines (Lewis, Leighfield and Cox 2000; Robins, Davies and Dumpleton 2008; Farr *et al.* 2016). With the exception of a cultivation-based study investigating moderate acidophiles in which isolates closely related to the thiosulfate-oxidizing *Thiomas thermosulfata* were enriched (Hallberg and Johnson 2003), the microbial communities of these ochreous deposits have not been investigated. Furthermore, the impacts of these communities on the fate of contaminants and the seasonal dynamics of microbial communities at these sites remain poorly understood.

Therefore, the aims of this study were to investigate the changes in the bacterial community structure according to spatial, temporal and environmental factors within an Fe(III)-rich deposit at an abandoned coal mine, Ynysarwed, in the SWC. This site is of particular interest due to the initial acidic and polluted discharge outburst (pH 3.2; 200–400 mg Fe L^{-1}) following a rebound in the water table in 1993 which resulted in the pollution of the local hydrological system (Younger 1997), and also the occurrence of the Fe(II)/Fe(III) (oxyhydr)oxide green rust found in the ochreous deposits (Bearcock *et al.* 2007). A high-resolution sampling strategy was employed for geochemical and bacterial 16S rRNA gene sequence analysis. Samples were collected from nine locations within the ochreous deposit from both the upper and lower layers of sediment. Our results show that bacterial communities within the Fe(III)-rich deposit are dynamic and vary both spatially and temporally with several operational taxonomic units (OTUs) closely related to known Fe-cycling bacteria; their activity and potential influence on biogeochemical cycling and pollutant sequestration are discussed.

METHODS

Field site

The SWC is an elongate, synformal structure of Carboniferous Coal Measures ~35 km north-south and ~80 km east-west covering an area of ~2690 km^2 (Bearcock *et al.* 2007; Farr *et al.* 2016) (Fig. 1). The geology of the region consists of faulted mudstones, sandstones, siltstones and coals of the Lower, Mid-

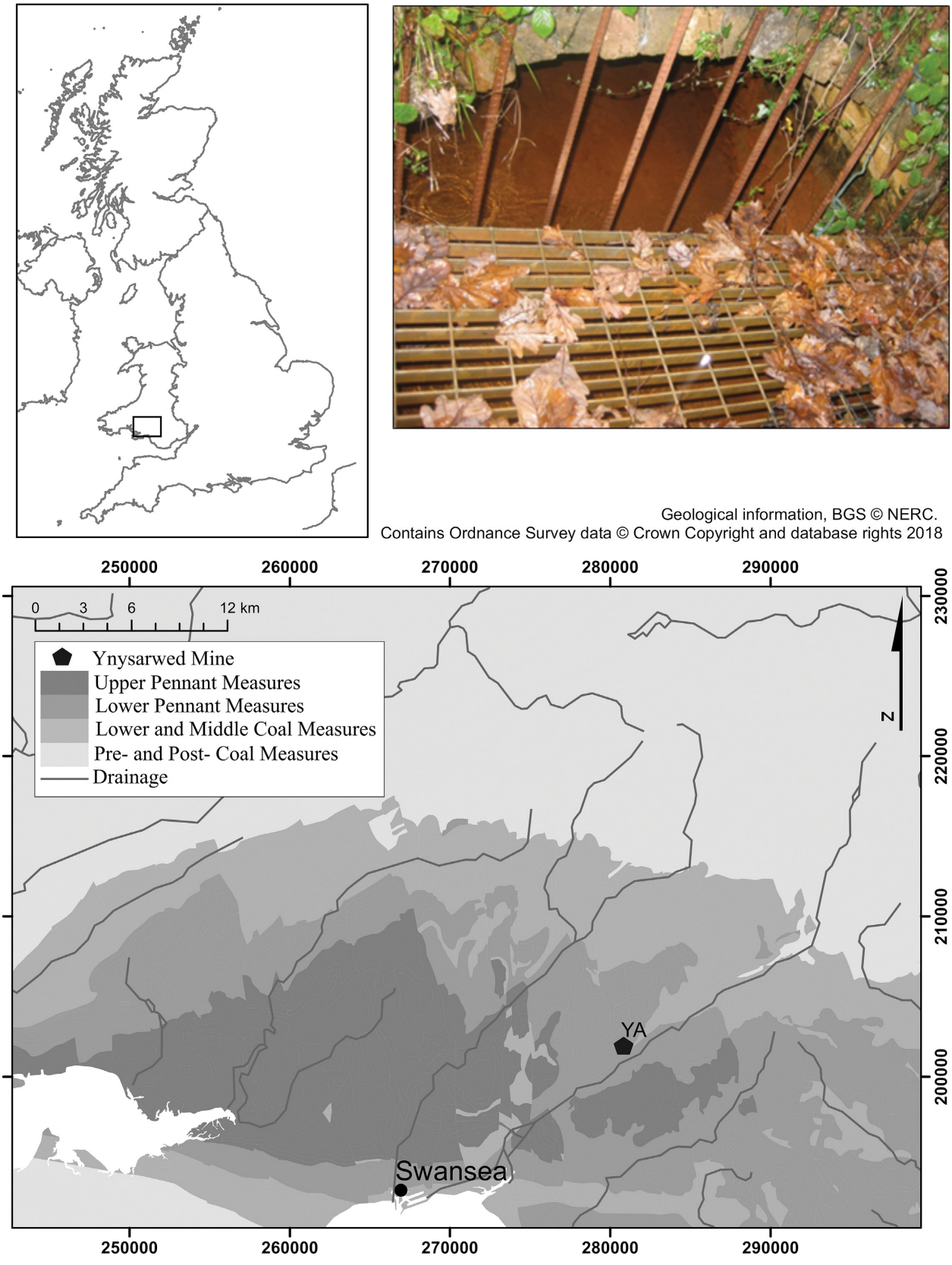

Figure 1. Sampling location at the Ynysarwed mine adit in the SWC, UK.

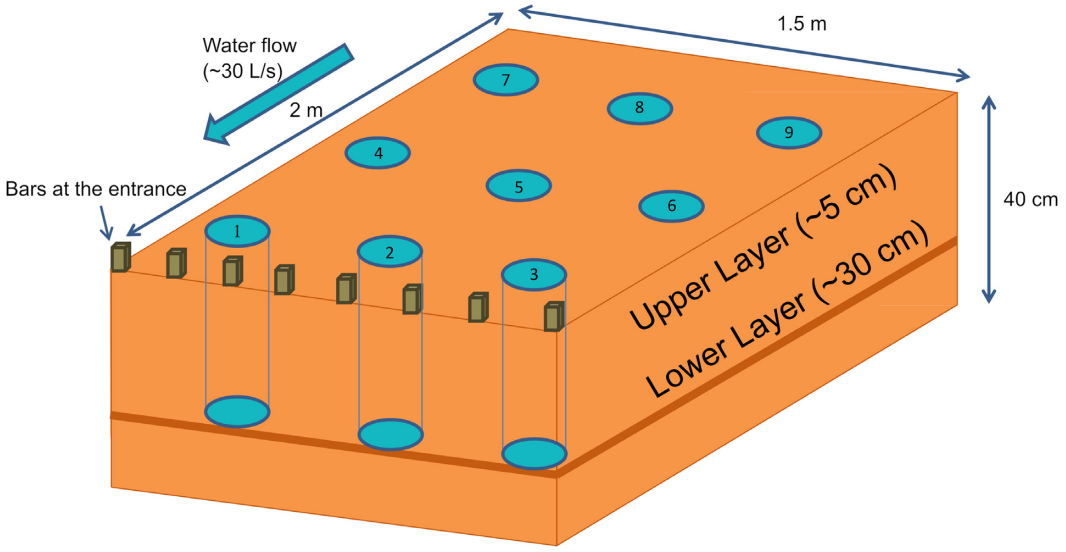

Figure 2. Schematic of high-resolution sampling strategy within the Fe-rich deposit at the Ynysarwed mine adit in the SWC, UK.

dle, and Upper Coal Measures deposited during the Westphalian Stage (Evans, Watkins and Banwart 2006). This is underlain by the Namurian age Marros Group, previously known as the Millstone Grit Series (Waters *et al.* 2009), and the Carboniferous Limestone Beds. Many coal seams in this area were deposited under marine conditions (Davies, Guion and Gutteridge 2012) and consequently have high pyrite content of around 2–4% (Evans, Watkins and Banwart 2006).

The Ynysarwed mine adit (51°42′05.9‘N, 3°43′33.1’W) (Fig. 1) is situated in the Lower Neath Valley and during operation mainly worked the notoriously pyritic Rhondda No. 2 coal seam of the Upper Coal Measures. Although the mine water pH is ∼6, the total dissolved Fe concentrations are greater than the Water Framework Directive guideline value (<1 mg L^{-1}) and elevated concentrations of total As in the water (up to 30 μg L^{-1}) have been measured at the mine.

Samples were collected for geochemical and molecular biological analysis in autumn (October 2011), winter (February 2012) and summer (July 2012). Nine locations (30–40 cm between locations) within the Fe(III)-rich deposit (total depth ∼40 cm) were selected with samples collected from the upper (∼5 cm) and lower (∼30 cm) layers of sediment from these locations (Fig. 2).

Geochemical analysis

Several physico-chemical parameters were measured in the field using unfiltered water including pH, Eh, conductivity and temperature. pH and Eh were measured using a calibrated HANNA HI 9025 microcomputer; for pH determination a calibrated VWR probe was used (pH meter accuracy ±0.01 pH units), and for Eh a Pt wire combination sensor was used (Eh meter accuracy ±1 mV). Temperature and conductivity were measured using a calibrated HANNA HI 98 312 Tester (conductivity range 0–20 mS/cm ± 2% of measured value).

Mine water samples collected from the entrance of the adit were filtered immediately in the field through a 0.22 μm cellulose nitrate membrane filter (Whatman, Maidstone, UK) and were either acidified (pH <2) for cation analysis or left nonacidified for anion analysis. Samples were transported in a cool box to the laboratory (<6 hours) where they were then stored at 4°C until analysis. Analysis of cations in solution was conducted on duplicate samples either on a Perkin Elmer AAnalyst 400 (PerkinElmer Inc., Waltham, MA, USA) atomic absorption spectrophotometer instrument or on an Agilent 7700x ICP-MS (Agilent, Santa Clara, CA, USA) using tellurium or ruthenium as the internal standard. Analysis of anions was conducted on duplicate samples on a Dionex DX 100 ion chromatograph (Thermo Scientific, Sunnyvale, CA, USA) with an IonPac AS4A-SC analytical column and was analyzed within one week of sample collection.

Sediment samples for geochemical analysis were collected using a clean, sterilized plastic scoop into sterile 50 mL Falcon tubes (Thermo Fisher Scientific Inc., UK). Each tube was filled quickly leaving no headspace to avoid changes in the sediment chemistry and was transported in a cool box back to the laboratory and stored at 4°C until analysis. Samples were subjected to centrifugation to remove excess water before being air-dried, sieved <150 μm and sent to the British Geological Survey (BGS), Keyworth, UK, for analysis of a suite of elements by ICP-MS (Agilent 7500cx quadrupole). A 0.25 g subsample of material was digested in perfluoroalkoxy (PFA) beakers with a mixture of concentrated hydrofluoric (47–51%), perchloric (46–49%) and nitric acid (67–69%) to a final volume of 25 mL and diluted 40-fold prior to analysis. The final concentration of the nitric acid following dilution was 5%, with trace amounts of hydrofluoric and perchloric acids. An internal standard solution containing scandium, germanium, rhodium, indium, technetium and iridium was added to the samples and instrument calibration standards. The standard reference material BGS-102 (BGS, Ironstone soil, UK) was used as the certified reference material (Wragg 2009).

The Fe(II) weight % in the sediment was measured using a modification of Wilson’s (1955) classical titration method as described in Bearcock *et al.* (2007). Porewater was extracted from the sediment by centrifugation (5000 x *g* for 10 minutes) and subsequently filtered (<0.2 μm; Whatman cellulose nitrate membrane). The dissolved Fe(II) content of the pore water was determined using the Ferrozine assay according to Stookey (1970) and measured on a Perkin Elmer UV–Vis spectrophotometer at 562 nm. The pH and weight % of organic matter (OM) in the sediment was determined by analysis at the BGS. Briefly, soil pH was determined by mixing a 5 g subsample of sieved sediment with

a freshly prepared 0.1 M $CaCl_2$ solution at a ratio of 1:2.5 (w/v). The slurry was stirred for 5 minutes and allowed to settle for at least 15 minutes before the pH measurement was determined using a calibrated pH meter. To determine the weight percentage of OM, the method of loss on ignition (LOI) was used. A 1 g subsample of sediment was weighed into a crucible (that had previously been weighed) and oven dried at 105°C for at least 4 hours. After cooling in a desiccator, the crucible and sediment were weighed again before being heated in a furnace at 450°C for at least 4 hours. Once cooled, the crucible and sediment were weighed again and the weight percentage of OM in the sediment was calculated.

Mineralogical analysis

To determine the mineralogy of the ochreous sediment—specifically the Fe minerals present—samples were analyzed by X-ray diffraction (XRD) and environmental scanning electron microscopy (ESEM). For ESEM, samples do not have to be dried and this method was selected to avoid any artificial changes that may occur within the sample during the drying process. For XRD analysis, an air dried sample of the sediment was gently disaggregated in an agate pestle and mortar and the powder was loaded onto a poly(methyl methacrylate) sample holder. The sample was analyzed using a Bruker D8 Advance X-ray diffractometer (Bruker AXS Inc., Madison, WI, USA) with a Vantec Super Speed detector and Cu Kα radiation (1.542Å). The system was set up with a step size of 0.007° 2θ and the scan speed was 0.01 seconds per step. The results were analyzed using the Diffrac.EVA software (Bruker AXS Inc., Madison, WI, USA). Analysis of samples by ESEM took place at the School of Earth and Environmental Sciences at the University of Manchester, UK, using a Philips XL30 ESEM-FEG (Philips, Eindhoven, Netherlands) instrument. Slurried samples were mounted onto 12.7 mm (0.5 inch) aluminium stubs using double-sided adhesive tape in an anoxic chamber (100% N_2) to avoid oxidation of the sample during preparation. Samples were transported within an airtight, oxygen-free container before being loaded into the instrument. Samples were analyzed at pressures between 0.5 and 0.6 torr using an accelerating voltage of 20 kV.

Microbiological sampling

Sediment samples for microbiological analysis were collected using a clean plastic scoop. A sterile spatula was used to transfer an aliquot of the scooped sample into a sterile 50 mL Falcon tube. The tubes were filled to avoid headspace and thus the introduction of oxygen into the sample and stored in the dark at ~4°C while being transported back to the laboratory and stored at −20°C prior to DNA extraction.

High-throughput semiconductor amplicon sequencing of partial 16S rRNA genes

Community DNA was extracted using the PowerSoil DNA extraction kit (MO BIO Laboratories Inc., CA, USA) according to the manufacturer's instructions. Samples—a total of 54–were then amplified by polymerase chain reaction (PCR) for semiconductor sequencing using the 27F (5′-AGAGTTTGATCMTGGCTCAG) (Lane 1991) and 357R (5′-CTGCTGCCTYCCGTA) (Klindworth *et al.* 2013) bacterial primer combination spanning the V1–V2 hypervariable region of the 16S rRNA gene. Sequencing adapters and barcodes (Whiteley *et al.* 2012) were incorporated into the forward and reverse primers. Amplicons were cleaned using the AmPure® XP PCR purification kit (Beckman-Coulter, MA, USA). DNA concentrations were measured using a NanoDrop ND-1000 UV-visible spectrophotometer and samples were normalized before pooling. The quality of the cleaned amplicons was tested by running the samples through an E-Gel® SizeSelect 2% Agarose gel on the E-Gel System (Life Technologies Ltd, Paisley, UK) and DNA fragments smaller than 400 bp were removed. The DNA was quantified on an Agilent 2100 Bioanalyzer with a high sensitivity DNA chip (Agilent Technologies UK Ltd, Stockport, UK) and diluted to 26 pmol L^{-1} in preparation for emulsion PCR. Emulsion PCR was conducted using the Ion PGM Template OT2 Reagents 400 kit 2.0 according to the manufacturer's guidelines on an Ion One Touch 2 System and was set up as per the manufacturer's guidelines (Life Technologies). Finally, the emulsion PCR amplified solution was loaded onto an Ion 316 Chip and run on the Ion Torrent PGM sequencer (Life Technologies) at the Institute of Biological, Environmental and Rural Sciences, Aberystwyth University, UK. The data were subjected to quality filtering (Ion Torrent default quality score setting <15 over a window size of 30 nt) before the data were exported as FASTQ files.

Sequences were analyzed using QIIME v.1.7.0 (Caporaso *et al.* 2010b). Briefly, the demultiplexed FASTQ files were labeled and filtered to remove any sequences smaller than 300 bp. The samples were then clustered into operational taxonomic units (OTUs) (default settings of 0.97 sequence similarity) using the UCLUST algorithm (Edgar 2010). A representative OTU was identified using the Greengenes database v.13_8 (DeSantis *et al.* 2006) using the Ribosomal Database Project (RDP) classifier algorithm (Cole *et al.* 2009) at 97% sequence similarity. The sequences were aligned against the Greengenes reference core imputed alignment (available from Greengenes website) using the PyNAST alignment method (Caporaso *et al.* 2010a). Following this, the data were checked for chimeric sequences using ChimeraSlayer (Haas *et al.* 2011) available in QIIME before they were removed via filtering. To visualize the data OTU tables were constructed and different filtering techniques (e.g. removal of singletons and sequences that accounted for <0.1% of the total microbial community) were used. In total, over 2 million reads were generated for the 54 samples. A read count heatmap generated in QIIME was exported to MS Excel to produce graphical plots. Raw data have been deposited at the sequence read archive (SRA) under project number PRJNA521102.

Statistical analyses

Environmental and microbiological data were exported into PRIMER software (version 6.1.12; Primer-E, Ivybridge, UK) with the PERMANOVA+ (version 1.0.2) add-on for statistical analysis. Environmental data were normalized and a Euclidean distance matrix constructed. For microbiological samples, data from the read count heatmap produced in QIIME was exported to MS Excel and the relative abundance of the OTUs as a percentage of the total bacterial community calculated. A Bray–Curtis resemblance matrix was constructed using fourth root transformed relative abundance data. PERMANOVA (Anderson 2001; Anderson and Willis 2003) was conducted using default settings with 9999 permutations for single factor analysis and reduced permutations for multifactor analysis while canonical analysis of principal coordinates (CAP) in PERMANOVA+ was conducted using default settings. Alpha diversity metrics including Chao1 (Chao 1984), Gini Index (Wittebolle *et al.* 2009), Good's Coverage (Good 1953), Observed Species (Kuczynski *et al.* 2011) and the Shannon Index (Shannon 1948) were calculated using the QIIME workflow scripts.

Table 1. General overview of geochemical parameters at the Ynysarwed mine site for the mine water, sediment and sediment porewater. Samples were collected in autumn (October 2011), winter (February 2012) and summer (July 2012). Sediment and porewater data show mean values for 18 samples collected at each timepoint. Bdl: below detection limit.

Parameter	Sample type	Mean (min—max)		
		Autumn	Winter	Summer
pH	Mine Water	6.2	6.1	6.3
Temperature (°C)		13.8	12.3	15.6
Eh (mV)		8.6	14.2	37.5
Conductivity (μS cm^{-1})		1212	1131	1173
Fe^{total} (mg L^{-1})		64.5 ± 1.9	55.3 ± 1.7	47.1 ± 1.4
Ca (mg L^{-1})		148 ± 1.9	140 ± 1.8	154 ± 2.0
Mg (mg L^{-1})		73.7 ± 2.5	72.4 ± 2.5	70 ± 2.4
Na (mg L^{-1})		74.5 ± 2.6	72 ± 2.5	77.5 ± 2.7
K (mg L^{-1})		19.8 ± 0.6	16.4 ± 0.5	21.2 ± 0.6
As^{total} (ug L^{-1})		19.5 ± 0.3	27.3 ± 0.4	29.7 ± 0.4
SO_4^{2-} (mg L^{-1})		352 ± 7.7	931 ± 20.5	844 ± 18.6
NO_3^- (mg L^{-1})		bdl	bdl	bdl
HCO_3^- (mg L^{-1})		248 ± 6.1	40 ± 0.1	109 ± 2.27
pH		5.3 (5.2–5.4)	6.3 (6.2–6.4)	6.3 (6.1–6.4)
Fe (%) in sediment		42.5 (38.4–48.1)	57.4 (48.7–63.7)	56.6 (52.7–61.1)
As in sediment (mg kg^{-1})	Sediment	1868 (1410–2252)	1228 (937–1356)	1230 (872–1439)
Ca in sediment (mg kg^{-1})		512 (211–2110)	2722 (1433–5092)	2195 (1361–3337)
Organic matter (%)		16.2 (12.5–34.3)	11.1 (9.9–12.5)	6.5 (5.8–9.9)
Fe(II) in porewater (mg L^{-1})	Pore Water	33.3 (19.9–47.1)	39.3 (13.2–49.5)	22.9 (<1–60.1)

Distance-based linear modeling was used to investigate the relationship between changes in bacterial community composition and environmental variable predictors using the PRIMER software. Environmental parameters included sediment digestion data, OM content, pH and Fe(II) porewater data.

PHREEQC geochemical modeling

PHREEQC v2.18 (Parkhurst and Appelo 1999) geochemical modeling software and the WATEQ4F database (Ball and Nordstrom 1991) were used to test the analytical quality and completeness of the geochemical data set (electrical balance variation <0.1%). The saturation index of various minerals and the speciation of contaminants of interest were also determined.

RESULTS

Geochemical analysis

Generally, the pH of the water flowing above the sediment remained circumneutral throughout the sampling period (pH ~6.2) (Table 1). For all sampling seasons the concentration of total Fe in the mine water remained consistently elevated (>47 ± 1.4 mg L^{-1}) and was greatest in autumn while the concentration of total As was greater in summer at 29.7 ± 0.4 μg L^{-1} (Table 1). PHREEQC analysis showed that up to 99% of the total As and >99% of the total Fe were present in the their reduced forms.

Iron was the major component in the sediment (up to 64%) with the lowest values seen in autumn and the highest in winter and summer (Table 1; Table S1, Supporting Information). The same was also true for the pH of the sediment (Table 1). Conversely, while the As in sediment was elevated throughout (>1200 mg kg^{-1}) it was highest in autumn and lowest in winter and summer (Table 1). The OM weight % of the sediment varied seasonally with the greatest OM content observed during autumn (mean of 16%; Table 1) before decreasing slightly in winter and again in summer (mean of 7%). The greatest percentage of OM was observed during autumn at location 4 in the upper sediments, along the left side of the deposit (Fig. 2), and was present at double the concentration of the surrounding samples at 34% (Table S1, Supporting Information). Similar to the OM results, Fe(II) concentrations in porewater were also typically higher in autumn and winter (Table 1) and had decreased by the summer apart from a localized area in the center of the deposit (mean Fe(II) concentration 52.5 mg L^{-1} for locations 4, 5, 6 and 8 in the lower sediments). Generally, for all months samples at the front of the sampling grid (i.e. locations 1–3) and in the upper sediments had lower Fe(II) porewater concentrations (Fig. 2; Table S1, Supporting Information).

Mineralogical analysis

Identification of the sediment by XRD showed the occurrence of the Fe(III) (oxyhydr)oxide mineral goethite (α-FeOOH) at the mine site and this was true for all sediment samples collected between autumn and summer (Figure S1, Supporting Information). ESEM images show poorly crystalline Fe minerals and twisted *Gallionella*-like stalks (e.g. Ionescu *et al.* 2015; Fabisch *et al.* 2016) as well as hollow structures reminiscent of biogenic Fe(III) mineral morphotypes formed by other Fe(II)-oxidizing bacteria (e.g. Fleming *et al.* 2011, 2014; Chan *et al.* 2016) (Fig. 3).

16S rRNA gene sequencing profiles

The results for the 16S rRNA gene sequencing of 54 samples from nine locations in the upper and lower deposit from the months of autumn, winter and summer are shown in Fig. 4. Results are discussed in relative bacterial 16S rRNA sequence abundance of OTUs as a proportion of the total number of reads per sample.

Phylogenetic diversity

Samples were analyzed for within-sample diversity (alpha) and between-sample diversity (beta) at OTU level (Table 2). A calcu-

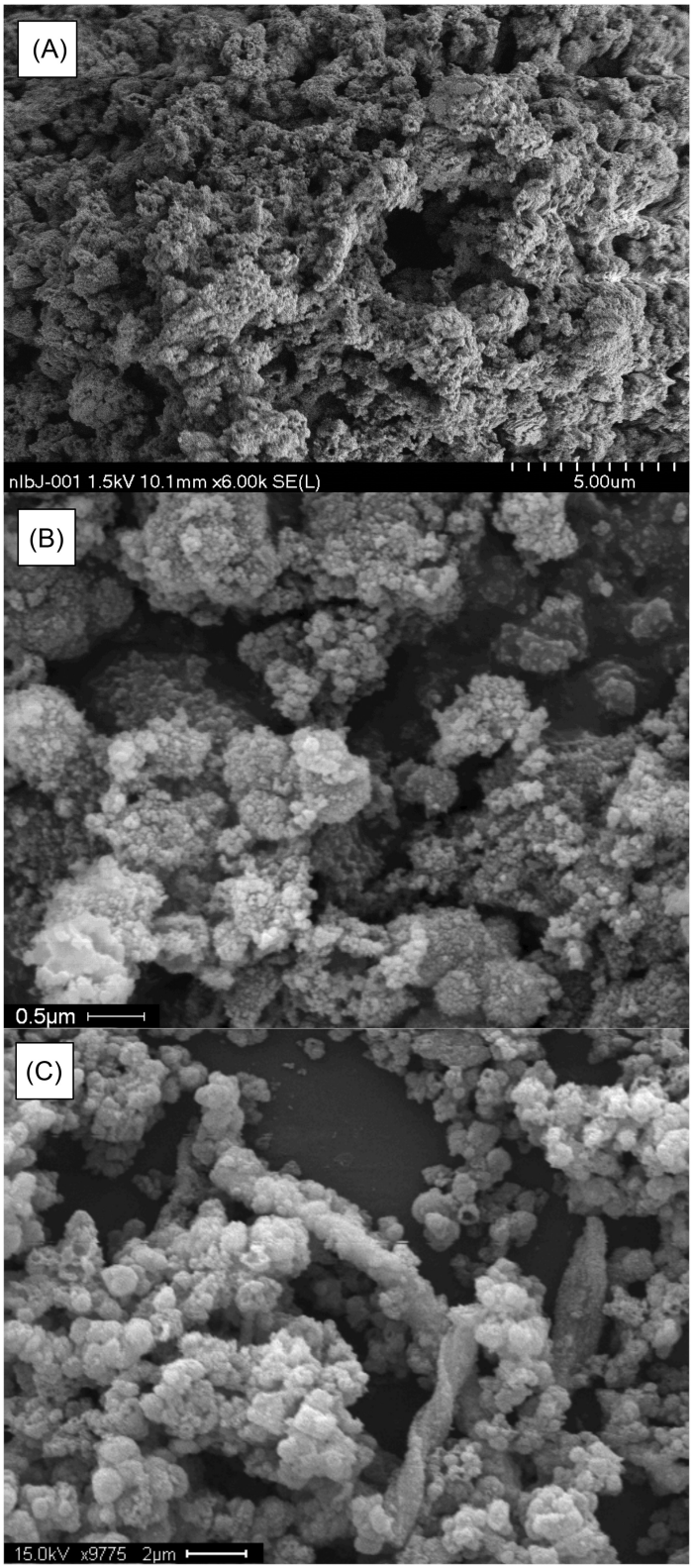

Figure 3. Electron microscopy micrographs of natural precipitates at the Ynysarwed mine adit showing poorly crystalline Fe minerals by **(A)** SEM, **(B)** ESEM (high vacuum) and **(C)** ESEM (high vacuum) showing Fe minerals and twisted *Gallionella*-like stalks.

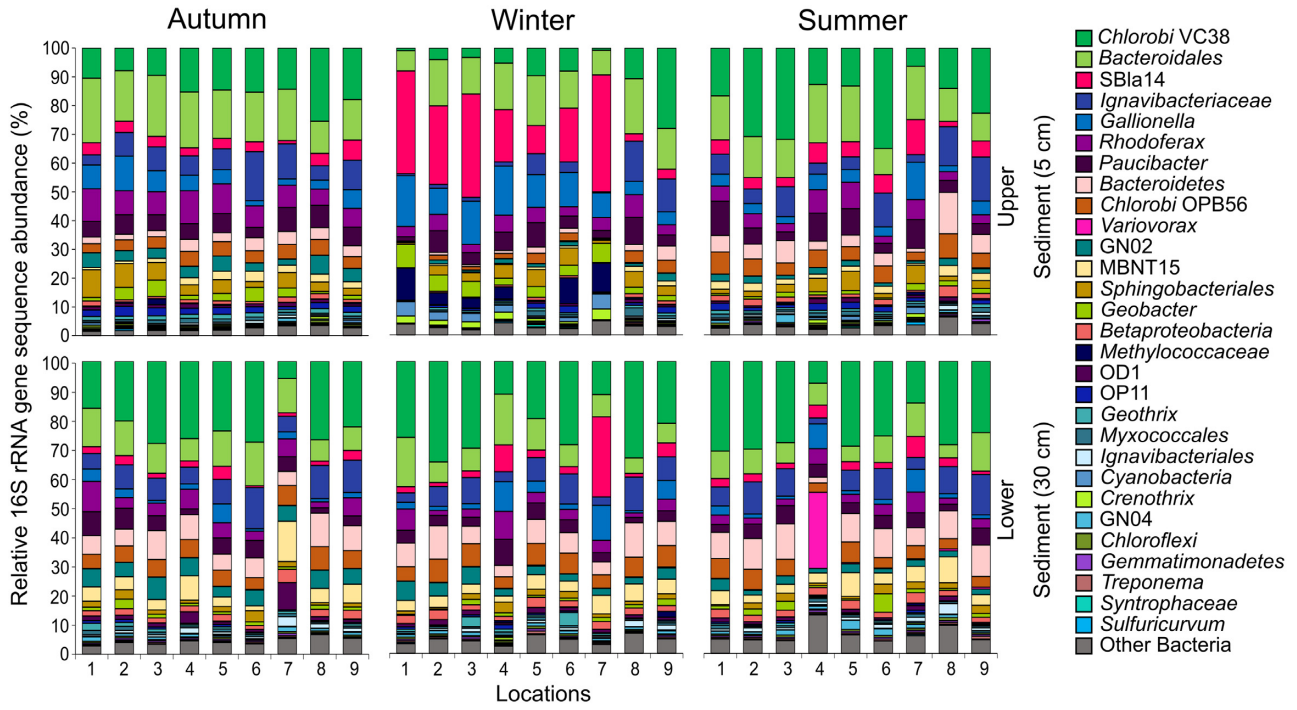

Figure 4. Relative 16S rRNA gene sequence abundance of bacterial groups in samples collected from the Ynysarwed mine at locations 1 to 9 in the upper (5 cm depth) and lower (30 cm depth) sediments in autumn (October 2011), winter (February 2012) and summer (July 2012). Bacterial groups were produced by clustering OTUs together based on their lowest level classification following QIIME analysis.

Table 2. Summary results for alpha diversity metrics for all 54 samples collected from the Ynysarwed mine adit calculated using the QIIME software package. (Note: Shannon values were converted from the QIIME output as the software calculates the metric to log base 2 not the natural log. Therefore, all output values were multiplied by 0.69315.)

Alpha diversity metric	Mean	Minimum	Maximum	Median
Chao1	93.3	80.2	98.3	94
Good's Coverage	100	100	100	100
Observed Species	92.3	79	95	93
Gini Index	0.7	0.6	0.8	0.7
Shannon	3.3	2.8	3.7	3.3

lation of Good's Coverage revealed that all samples had coverage of 100. The mean Shannon–Weaver diversity index for all samples was 3.3 and further analysis of samples by month did not deviate greatly from this value (range 3.2–3.3).

Taxonomic composition

At phylum level, the *Proteobacteria* were the most dominant and accounted for 34% of the total bacterial community (mean value for all 54 samples; Dataset S1, Supporting Information). The majority of the remaining population was comprised of bacteria affiliated with the *Chlorobi* (33%) and *Bacteroidetes* (21%) phyla. Also present were lineages affiliated to the phyla *Acidobacteria*, *Actinobacteria* and *Nitrospirae*, though at a much lower abundance (Dataset S1, Supporting Information). Certain sequences represented lineages that were unidentifiable at phylum level and accounted for 0.7 to 3.7% of the total community. At class level, the *Betaproteobacteria* were the most dominant and represented 25% of total community on average. The *Chlorobi* were mainly represented by BSV6, *Ignavibacteria* and OPB56. At genus level, the *Betaproteobacteria* were mainly comprised of several OTUs from the family *Comamonadaceae* including *Paucibacter* and *Rhodoferax*. Also, within the *Betaproteobacteria* were OTUs from the order SBla14 and the Fe(II)-oxidizing genus *Gallionella*, while the order *Desulfuromonadales* from the *Deltaproteobacteria* was represented entirely by the genus *Geobacter* which contains known Fe(III)-reducing bacteria (Dataset S1, Supporting Information).

Variations in taxonomic composition according to depth and location

Bacterial communities were sorted according to the sampling depth and location regardless of the sampling month. At OTU level, there was no significant difference between locations for any month ($P > 0.05$; Fig. 5A); however, highly significant differences between sample depths were observed ($P = 0.0002$, 0.0001 and 0.0054, Pseudo-$F = 15.54$, 19.47 and 5.61 for autumn, winter and summer, respectively). In the upper sediment, the dominant phyla were *Proteobacteria* (40%), *Chlorobi* (27%) and *Bacteroidetes* (23%) (Figure S2, Supporting Information). The same three phyla were dominant in the lower sediments; however, the relative abundance of *Proteobacteria* decreased (27%), while *Chlorobi* increased (40%) and *Bacteroidetes* remained consistent (20%). Pairwise analysis for each of the three main phyla according to depth showed significant differences ($P < 0.05$; Table S2, Supporting Information). OTUs within the order SB1a14 were more abundant in the upper sediments (ranging 1–40%) compared to the lower sediments (ranging 0.6–27%). The same was also true for OTUs from the genus *Gallionella* (Dataset S1, Supporting Information). OTUs classified as the Fe(III)-reducing bacteria-containing genus *Geothrix* were evenly distributed (though at low abundance, ~1%).

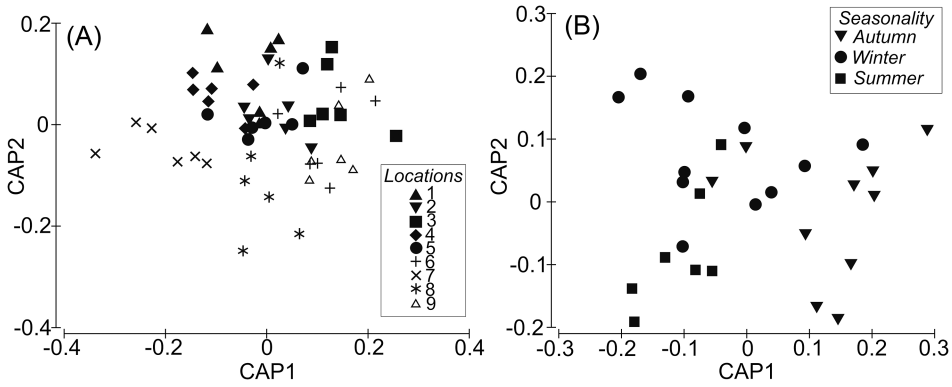

Figure 5. Bacterial community diversity according to **(A)** locations and **(B)** seasons based on Bray–Curtis distances of fourth root transformed abundance data.

Seasonal variations in taxonomic composition

Generally, the community compositions for autumn and summer were the most similar based on the relative abundance of the most dominant phyla (Figure S3, Supporting Information). Mean values for each month (upper and lower sediments combined) showed that the abundance of OTUs from the phylum *Proteobacteria* were similar in autumn and summer (28–29%), which was also true for the *Chlorobi* (34–38%) (Figure S3, Supporting Information). Samples collected during winter, however, displayed a different composition and an increase in *Proteobacteria* (to 42%) and a concomitant decrease in *Chlorobi* (to 27%) was observed. Pairwise analysis of *Proteobacteria*- and *Chlorobi*-affiliated OTUs according to months showed significant ($P < 0.05$) differences between autumn versus winter and winter versus summer, but not between autumn versus summer (Fig. 5B; Table S2, Supporting Information). A similar clustering of samples was observed when samples were analyzed with nonmetric dimensional scaling (nMDS) at OTU level (Figure S4, Supporting Information). Further investigation of the winter samples revealed that the increase in *Proteobacteria* mainly occurred in the upper sediments (56%) compared to the lower sediment (29%). One of the greatest variations in the *Proteobacteria* occurred within the *Betaproteobacterial* order SB1a14 which increased up to 40% in certain samples during winter (Fig. 4), before decreasing again in summer. The same was also true for *Gallionella*-affiliated OTUs. The decrease in *Chlorobi* in winter was particularly apparent in the order VC38 (Fig. 4) and the relationship between the relative abundance of the *Chlorobi* order VC38 and *Betaproteobacteria* order SBla14 appeared to be closely linked (Fig. 6).

Differences in community structure between neighboring samples were also apparent (Fig. 4). However, at OTU level these differences were not statistically significant during any month ($P > 0.3$). In relation to the grid sampling strategy, a general pattern was observed: between autumn and winter an increase in the relative abundance of *Proteobacteria*-affiliated OTUs, especially order SBla14, occurred within upper sediment samples collected along the front and left side of the adit (locations 1–7; Fig. 2). This substantial increase in order SBla14 was also observed in the lower sediments, though only in one sample at location 7. An increase in the genus *Geobacter* was observed in upper sediment samples 1–7 during winter (Fig. 4), for example, the mean relative abundance ($n = 7$) during winter was 5% compared to 3 and 1% in autumn and summer, respectively. This was also true for the genus *Gallionella*, for example, at location 1 in the upper sediments the relative abundance increased from 8% in autumn to 18% in winter before decreasing to 4% in summer. Within the lesser represented taxa seasonal variations were also evident with a large increase in a single OTU affiliated to the species *Variovorax paradoxans* (99% 16S rRNA gene identity). At location 4 in the lower sediments during summer, the relative abundance of this OTU was 26% while for the remaining samples it was <1%.

DISCUSSION

Impacts of historical mining on water quality

The occurrence of precipitated Fe(III) minerals at the Ynysarwed mine site is indicative of the dissolution of pyrite that is present in the worked coal seams within the mine (Evans, Watkins and Banwart 2006). During aerobic working conditions, highly soluble secondary minerals known as efflorescent salts (Nordstrom and Alpers 1999) such as melanterite ($FeSO_4{\cdot}7H_2O$), which has been found in many mines in the SWC (Bevins 1994), likely formed on the surface of the seams (Robins, Davies and Dumpleton 2008). Dissolution of these salts and further pyrite oxidation caused either by microbially mediated processes (Quatrini and Johnson 2018) or chemically by strong oxidants such as Fe^{3+} (Johnson and Hallberg 2003) result in Fe- and sulfate-rich mine waters as shown in the water chemistry data. Furthermore, the elevated total As concentrations may indicate the presence and biodegradation of As-bearing ores such as arsenopyrite, while the elevated Ca and Mg concentrations are due to the occurrence of carbonate rocks, which is in agreement with the local geology. The relationship between Fe minerals and contaminants is well documented, e.g. Dzombak and Morel (1990) and several studies have shown that Fe(III) (oxyhydr)oxides are capable of sequestering As from solution through absorption or coprecipitation at circumneutral pH (e.g. Adra *et al.* 2013; Sowers *et al.* 2017) which explains the elevated concentrations of total As in the sediment.

Bacterial taxa associated with iron cycling

Lineages affiliated with those known to contain Fe-cycling microbes were found at comparatively high relative abundances that changed seasonally. OTUs affiliated to known Fe(III)-reducing bacteria genera include *Geothrix, Geobacter* and *Rhodoferax*. An OTU demonstrating 99% 16S rRNA gene identity to *Rhodoferax ferrireducens* (Finneran, Johnsen and Lovley 2003), a facultative anaerobe, was present in all samples. *Geobacter* spp. are known Fe(III) reducers capable of coupling organic carbon oxidation to Fe(III) reduction (Lovley 1997; Islam *et al.* 2004). OTUs affiliated to the *Geobacter* genus demonstrated 96% 16S rRNA gene identity across the sequenced region to *Geobacter psychrophilus* (Nevin *et al.* 2005) and 98% 16S rRNA gene similarity to clones of subsurface *Geobacter* communities stimulated

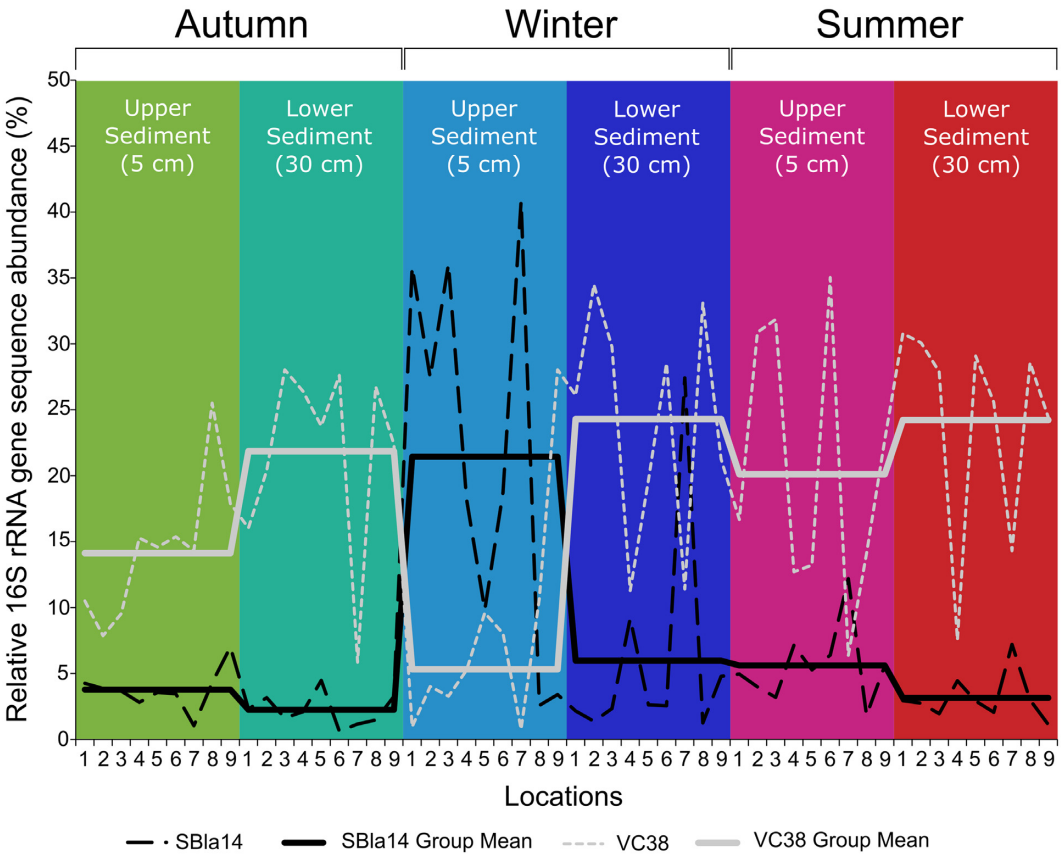

Figure 6. A bloom of the *Betaproteobacterial* order SB1a14 and a concomitant decrease in *Chlorobi* order VC38 in the upper (5 cm) sediment layer during winter (February 2012). Samples were grouped according to month and depth and a mean abundance ($n = 9$) for both taxa was calculated. Numbers refer to the location of the sample.

by acetate addition to a uranium-contaminated aquifer (Elifantz *et al.* 2010).

Lineages affiliated to those containing known Fe(II)-oxidizing bacteria were also present in relatively high abundances in the sediment. Microaerophilic Fe(II) oxidizers, such as *Gallionella* spp., exist at the redox boundary of opposing gradients of oxygen and Fe(II) (Emerson and Moyer 1997; Neubauer, Emerson and Megonigal 2002; Lueder *et al.* 2018). *Gallionella* spp. grow by using Fe(II) as the electron donor and oxygen as the electron acceptor (Hallbeck and Pedersen 1991). They have also been found to be surprisingly dominant under slightly acidic conditions (pH ~4) (Fabisch *et al.* 2013). The sequences of the representative OTUs identified as *Gallionella* spp. were verified by BLAST to identify the OTUs at species level. The most abundant *Gallionella*-related OTUs shared the greatest gene sequence identity with *Gallionella capsiferriformans* ES-2 (97–98% 16S rRNA gene sequence identity) (Emerson *et al.* 2013) although OTUs present at lower abundances (<1%) were not as similar (94–95%). The occurrence of Fe(II) oxidizers closely related to this species at heavy metal contaminated sites has already been documented (Fabisch *et al.* 2016). This may be explained by the presence of heavy metal efflux pumps found in the genome as well as genes for arsenic resistance (Emerson *et al.* 2013). The general greater relative abundance of microaerophilic *Gallionella*-related species in the upper sediments (5 cm depth) also suggests a vertically stratified redox gradient within the ochreous deposits, a phenomenon known to occur in Fe-cycling sediments (Duckworth *et al.* 2009). The *Betaproteobacterial* order SBla14, which consisted of three OTUs, increased substantially during winter in the upper sediments particularly at locations 1–7 at the front and left side of the adit. Further analysis of the dominant OTUs within this order showed 95–97% 16S rRNA gene similarity to the Fe(II)-oxidizing bacterium *Sideroxydans lithotrophicus* ES-1 (Emerson *et al.* 2013), and 99% 16S rRNA gene identity to clones obtained from 'iron snow' particles present in an acidic lignite mine lake (Reiche *et al.* 2011). While it is not possible to infer *in situ* microbial function from partial 16S rRNA gene sequence data, it can be hypothesized that the SBla14-affiliated OTUs are involved in Fe(II) oxidation. However, further isolation and physiological studies are required to determine this.

Ecological succession

This research shows clear evidence for ecological succession between two of the most abundant taxa at the field site. A concomitant change in the bacterial community was observed in members of the *Chlorobi* order VC38 and members of the *Betaproteobacteria* order SBla14 throughout the course of one year. *Chlorobi* VC38 OTUs dominated the communities in autumn; however, by winter *Betaproteobacteria* SBla14 OTUs were the most dominant. By summer, the community had returned to almost the same community observed in autumn the previous year demonstrating a cyclic transition between the two principal community members. It can be hypothesized that the increase in the *S. lithotrophicus*-related putative Fe(II) oxidizer from the order SBla14 during winter, especially in the upper sediments (up to 40%), is due to conditions favorable for microaerophilic Fe(II) oxidation. This is also evident in the increase in *Gallionella* for the same month. However, the role of OTUs related to the *Chlorobi* VC38 remains unknown. Further analysis of the OTUs

revealed little more information (closest cultured relative <91% similarity)—only that environmental clones with no hypothesized function from an acid-impacted lake were closely related (99% 16S rRNA gene similarity) (Percent *et al.* 2008). Members of the *Chlorobi* are known for growth via anoxygenic photosynthesis, coupling the fixation of CO_2 into biomass with the oxidation of reduced sulfur to replace the electrons lost from the photosystem during carbon assimilation (Overmann 2006). However, certain members of the *Chlorobi* phylum can grow by oxidizing Fe(II) (e.g. Crowe *et al.* 2017), the so called photoferrotrophs (see Bryce *et al.* 2018 for a comprehensive review). If this is the case, the temporal transition from the putative microaerophilic to an anoxygenic photoferrotrophic metabolism could represent a phenomenon that has yet to be described in circumneutral mine drainage environments. Currently, most photoferrotrophic isolates have originated from either freshwater sediment and lakes or marine sediments (Bryce *et al.* 2018). The occurrence of *Chlorobi* has been reported in 16S rRNA gene sequencing surveys of acid mine drainage (Volant *et al.* 2014; Mesa *et al.* 2017) and soils impacted by circumneutral mine drainage (Pereira, Vicentini and Ottoboni 2014) though at low abundance (<1%). It is possible that the high relative abundance for *Chlorobi*-affiliated OTUs at Ynysarwed represents a previously overlooked microbial metabolism in circumneutral mine drainage that can greatly impact pollutant turnover.

While the ecological function of the dominant *Chlorobi*-affiliated OTU at the Ynysarwed mine adit cannot be inferred from the partial 16S rRNA gene sequencing data currently available, it highlights the need for cultivation-based approaches to determine the metabolism of this particular bacterium, and may provide insight into the type of growth conditions to be tested (i.e. anoxygenic photoferrotrophy). This research demonstrates that there is likely a complex interplay between geochemical and microbial factors that result in a seasonal ecological succession, and further cultivation-dependent and metagenomics work could help to elucidate the role of the *Chlorobi* VC38- and *Betaproteobacteria* SBla14-affiliated bacteria.

Fluxes of substrates drive biogeochemical iron cycling

The OM content of the sediment varied seasonally and by location and is likely to reflect the deposition of fallen leaves from nearby deciduous trees during winter months. The particularly elevated concentration at location 4 in the upper sediments compared to other samples indicates that this localized influx of OM is the case. The occurrence of leaves in the sediment, particularly at the entrance of the adit, was noted several times during fieldwork. The concentration of Fe(II) in pore waters varied spatially and may be due to the influence of infiltrating oxygen from the atmosphere into the sediments. This is shown by the comparatively lower concentrations measured at the entrance of the adit at locations 1, 2 and 3. Conversely, the localized area of comparatively elevated concentrations of Fe(II) centered around location 5L may indicate the lack of oxygen infiltration to these parts. Another possibility is that the influx of organic carbon stimulated the reduction of bioavailable Fe(III) by Fe(III)-reducing microbes. Lineages affiliated to those known to be capable of Fe(III) reduction were detected at relatively high abundances within the sediment.

Although the greatest OM content was detected during autumn, the change in the bacterial community may not occur immediately. A possible reason for this includes a delay period created by the time necessary for the catabolism of the complex organic compounds by a certain taxon, or indeed several taxa, into more simple forms that can be used by other microbes. This, therefore, also suggests the presence of a syntrophic microbial community where microbes take advantage of the metabolic abilities of their syntrophic partner (Schink 2002; Stams and Plugge 2009). At location 4 during summer—the location with the greatest OM content measured in the study (in the upper sediments in autumn at ~34%)—an increase in an OTU affiliated to the bacterium *Variovorax paradoxus* (99% 16S rRNA gene sequence similarity) was observed in the lower sediments. This species, a member of the family *Comamonadaceae* within the *Proteobacteria* formerly known as *Alcaligenes paradoxus* (Davis *et al.* 1969; Willems *et al.* 1991), has numerous metabolic capabilities that are associated with important catabolic processes including the degradation of toxic and complex chemical compounds. These include the degradation of chitin, cellulose and humic acids (Satola, Wübbeler and Steinbüchel 2013). Several strains of *V. paradoxus* have been shown to participate in syntrophic relationships with other plant and bacterial species (Satola, Wübbeler and Steinbüchel 2013). The importance of this bacterium in the degradation process of OM and also its involvement in numerous syntrophic processes suggest that the increase in relative abundance is due to the addition of OM to the sediment.

The substantial bacterial community changes observed at locations 1–7 in the upper sediments during winter, specifically an increase in putative Fe(II) oxidizers from the order SBla14, are likely due to the formation of additional Fe(II) by Fe(III) reducers. Fe(III)-reducing bacteria have been shown to greatly impact and decrease the net Fe(II) oxidation rate in natural sediments due to their rapid reduction rates (Laufer *et al.* 2016a). This rapid reduction of Fe(III) would provide sufficient Fe(II) to support microbial microaerophilic Fe(II) oxidation and during that time an increase in the comparatively well characterized Fe(II)-oxidizing *Gallionella* was also observed. Furthermore, the occurrence of OM plays an important role in the stabilization of Fe(II) (Sundman *et al.* 2014; Bhattacharyya *et al.* 2018) by forming OM–Fe(II) complexes which have been found in a range of environments (Kleja *et al.* 2012; von der Heyden *et al.* 2014; Hopwood *et al.* 2015). Therefore, a decrease in abiotically oxidized Fe(II) either by molecular oxygen or through heterogenous Fe(II) oxidation (Park and Dempsey 2005; Melton *et al.* 2014) and an increase in OM–Fe(II) complexes could provide a more stable substrate available for use by Fe(II)-oxidizing bacteria. This, combined with a potential increase in the activity of Fe(III)-reducing bacteria, could explain the bloom in abundance of putative Fe(II)-oxidizing bacteria at the site.

Implications for contaminant dynamics

The formation, and also dissolution, of Fe(III) (oxyhydr)oxide minerals can have substantial impacts on contaminant and nutrient dynamics (Islam *et al.* 2004; Borch *et al.* 2010; Eickhoff *et al.* 2014). Therefore, the activity of Fe-cycling bacteria play a major role in the sequestration and release of contaminants, such as As, in the environment. Analysis of the sequence data showed a dramatic increase in OTUs from the *Betaproteobacterial* order SBla14, a putative Fe(II)-oxidizing bacterium related to *S. lithotrophicus* ES-1, as well as *Gallionella*-related OTUs during winter. This may have implications on the release of As from the mine site. As previously discussed, biogenic Fe(III) minerals are known strong sorbents and sinks for As (Hohmann *et al.* 2010; Sowers *et al.* 2017) and therefore a bloom in Fe(II)-oxidizing bacteria and subsequent Fe(III) biomineral production could increase the sequestration of As from the mine water. This

is not supported by the geochemical water chemistry data as the concentration of As in solution increased slightly through the sampling period. However, the processes, such as dissolution of As-bearing minerals and water retention times occurring within the flooded mine, upstream of the mine adit are unknown and might have masked the processes at the adit entrance.

CONCLUSIONS AND OUTLOOK

The geochemistry and relative bacterial 16S rRNA gene abundance of nine locations within an Fe(III)-rich deposit at an abandoned coal mine in the SWC showed clear differences between months, depths and locations. In autumn (October 2011) OTUs closely related to *Chlorobi* VC38 which could potentially be an anoxygenic photoferrotroph dominated; however, by winter (February 2012) the putative Fe(II)-oxidizing *Betaproteobacteria* SBla14 related to *S. lithotrophicus* bloomed to abundance. An increase in the well-described Fe(II) oxidizer *Gallionella* was also observed but to a lesser extent. By summer (July 2012), the community had returned to almost the same community observed in the previous autumn demonstrating a cyclic transition between the two principal community members, possibly related to the influx of OM to the sediment. This clear ecological succession highlights the importance of spatial and temporal sampling strategies when investigating environmental systems. The high relative abundance of the *Chlorobi*-affiliated OTUs that currently have no known ecological function indicates the importance and necessity of further investigations at this site, and also other sites in the SWC, to include cultivation-dependent and metagenomics approaches to determine their potential influence on contaminant and nutrient dynamics.

SUPPLEMENTARY DATA

Supplementary data are available at FEMSEC online.

ACKNOWLEDGMENTS

The authors thank Thomas Barlow and Amanda Gardner at the British Geological Survey (BGS) Inorganic Geochemistry Laboratories for geochemical analyses, Dr John Waters for assistance with ESEM, Dr Toby Wilkinson and Dr Susan Girdwood for assistance with semiconductor sequencing and Andrew Brown for assistance with geochemical analyses. Also, thanks to Dr Kevin Hallberg, Professor Barrie Johnson and Dr Gareth Griffith for helpful discussions.

FUNDING

This work was supported by and in part funded by the British Geological Survey University Funding Initiative PhD studentship (grant S188) and Aberystwyth University while AE acknowledges support from the Welsh Government and the Higher Education Funding Council for Wales via National Research Network Low Carbon, Energy and Environment GeoCarbCymru.

Conflict of interest. None declared.

REFERENCES

Adra A, Morin G, Ona-Nguema G *et al*. Arsenic scavenging by aluminum-substituted ferrihydrites in a circumneutral pH river impacted by acid mine drainage. *Environ Sci Technol* 2013;**47**:12784–92.

Anderson MJ. A new method for non-parametric multivariate analysis of variance. *Austral Ecol* 2001;**26**:32–46.

Anderson MJ, Willis TJ. Canonical analysis of principal coordinates: a useful method of constrained ordination for ecology. *Ecology* 2003;**84**:511–25.

Ball JW, Nordstrom DK, User's manual for WATEQ4F, with revised thermodynamic data base and test cases for calculating speciation of major, trace, and redox elements in natural waters. *Open-file report*. U.S. Geological Survey 1991.

Bearcock JM, Perkins WT, Dinelli E *et al*. Fe(II)/Fe(III) 'green rust' developed within ochreous coal mine drainage sediment in South Wales, UK. *Mineral Mag* 2007;**70**:731–41.

Bevins RE. *A Mineralogy of Wales*. Cardiff: National Museum of Wales Press, 1994.

Bhattacharyya A, Schmidt MP, Stavitski E *et al*. Iron speciation in peats: chemical and spectroscopic evidence for the co-occurrence of ferric and ferrous iron in organic complexes and mineral precipitates. *Org Geochem* 2018;**115**:124–37.

Borch T, Kretzschmar R, Kappler A *et al*. Biogeochemical redox processes and their impact on contaminant dynamics. *Environ Sci Technol* 2010;**44**:15–23.

Brammer H, Ravenscroft P. Arsenic in groundwater: a threat to sustainable agriculture in South and South-east Asia. *Environ Int* 2009;**35**:647–54.

Bryce C, Blackwell N, Schmidt C *et al*. Microbial anaerobic Fe(II) oxidation - ecology, mechanisms and environmental implications. *Environ Microbiol* 2018;**20**:3462–83.

Canfield DE. Reactive iron in marine sediments. *Geochim Cosmochim Ac* 1989;**53**:619–32.

Caporaso JG, Bittinger K, Bushman FD *et al*. PyNAST: a flexible tool for aligning sequences to a template alignment. *Bioinformatics* 2010a;**26**:266–7.

Caporaso JG, Kuczynski J, Stombaugh J *et al*. QIIME allows analysis of high-throughput community sequencing data. *Nat Methods* 2010b;**7**:335–6.

Chan CS, McAllister SM, Leavitt AH *et al*. The architecture of iron microbial mats reflects the adaptation of chemolithotrophic iron oxidation in freshwater and marine environments. *Front Microbiol* 2016;**7**:769.

Chao A. Nonparametric estimation of the number of classes in a population. *Scand J Stat* 1984;**11**:265–70.

Coby AJ, Picardal F, Shelobolina E *et al*. Repeated anaerobic microbial redox cycling of iron. *Appl Environ Microbiol* 2011;**77**:6036–42.

Cole JR, Wang Q, Cardenas E *et al*. The ribosomal database project: improved alignments and new tools for rRNA analysis. *Nucleic Acids Res* 2009;**37**:D141–5.

Crowe SA, Hahn AS, Morgan-Lang C *et al*. Draft genome sequence of the pelagic photoferrotroph chlorobium phaeoferrooxidans. *Genome Announc* 2017;**5**:e01584–16.

Cummings DE, Caccavo F, Fendorf S *et al*. Arsenic mobilization by the dissimilatory Fe(III)-reducing bacterium Shewanella alga BrY. *Environ Sci Technol* 1999;**33**:723–9.

Davies SJ, Guion PD, Gutteridge P. Carboniferous sedimentation and volcanism on the laurussian margin. *Geological History of Britain and Ireland*. 2nd edn, Chichester: Wiley-Blackwell, 2012, 231–73.

Davis DH, Doudoroff M, Stanier RY *et al*. Proposal to reject the genus Hydrogenomonas: taxonomic implications. *Int J Syst Bacteriol* 1969;**19**:375–90.

DeSantis TZ, Hugenholtz P, Larsen N *et al*. Greengenes, a chimera-checked 16S rRNA gene database and workbench compatible with ARB. *Appl Environ Microbiol* 2006;**72**:5069–72.

Dixit S, Hering JG. Comparison of arsenic(V) and arsenic(III) sorption onto iron oxide minerals: implications for arsenic mobility. *Environ Sci Technol* 2003;**37**:4182–9.

Duckworth OW, Holmström SJM, Peña J *et al*. Biogeochemistry of iron oxidation in a circumneutral freshwater habitat. *Chem Geol* 2009;**260**:149–58.

Dzombak DA, Morel F. *Surface Complexation Modeling : Hydrous Ferric Oxide*. New York: Wiley, 1990.

Edgar RC. Search and clustering orders of magnitude faster than BLAST. *Bioinformatics* 2010;**26**:2460–1.

Eickhoff M, Obst M, Schröder C *et al*. Nickel partitioning in biogenic and abiogenic ferrihydrite: The influence of silica and implications for ancient environments. *Geochim Cosmochim Ac* 2014;**140**:65–79.

Elifantz H, N'Guessan LA, Mouser PJ *et al*. Expression of acetate permease-like (apl) genes in subsurface communities of Geobacter species under fluctuating acetate concentrations. *FEMS Microbiol Ecol* 2010;**73**:441–9.

Emerson D, Field EK, Chertkov O *et al*. Comparative genomics of freshwater Fe-oxidizing bacteria: implications for physiology, ecology, and systematics. *Front Microbiol* 2013;**4**:254.

Emerson D, Moyer C. Isolation and characterization of novel iron-oxidizing bacteria that grow at circumneutral pH. *Appl Environ Microbiol* 1997;**63**:4784–92.

Emerson D, Scott JJ, Benes J *et al*. Microbial iron oxidation in the Arctic tundra and its implications for biogeochemical cycling. *Appl Environ Microbiol* 2015;**81**:8066–75.

Evans KA, Watkins DC, Banwart SA. Rate controls on the chemical weathering of natural polymineralic material. II. Rate-controlling mechanisms and mineral sources and sinks for element release from four UK mine sites, and implications for comparison of laboratory and field scale weathering. *Appl Geochemistry* 2006;**21**:377–403.

Fabisch M, Beulig F, Akob DM *et al*. Surprising abundance of Gallionella-related iron oxidizers in creek sediments at pH 4.4 or at high heavy metal concentrations. *Front Microbiol* 2013;**4**:390.

Fabisch M, Freyer G, Johnson CA *et al*. Dominance of "Gallionella capsiferriformans" and heavy metal association with Gallionella-like stalks in metal-rich pH 6 mine water discharge. *Geobiology* 2016;**14**:68–90.

Farr G, Sadasivam SManju, *et al*., Manju Low enthalpy heat recovery potential from coal mine discharges in the South Wales Coalfield. *Int J Coal Geol* 2016;**164**:92–103.

Faure G. *Principles and Applications of Geochemistry*. New Jersey: Prentice Hall, 1998.

Finneran KT, Johnsen C V, Lovley DR. Rhodoferax ferrireducens sp. nov., a psychrotolerant, facultatively anaerobic bacterium that oxidizes acetate with the reduction of Fe(III). *Int J Syst Evol Microbiol* 2003;**53**:669–73.

Fleming EJ, Cetinić I, Chan CS *et al*. Ecological succession among iron-oxidizing bacteria. *ISME J* 2014;**8**:805–15.

Fleming EJ, Langdon AE, Martinez-Garcia M *et al*. What's new is old: resolving the identity of leptothrix ochracea using single cell genomics, pyrosequencing and FISH. *PLoS One* 2011;**6**:e17769.

Gadd GM. Microbial influence on metal mobility and application for bioremediation. *Geoderma* 2004;**122**:109–19.

Good IJ. The population frequencies of species and the estimation of population parameters. *Biometrika* 1953;**40**:237–64.

Haas BJ, Gevers D, Earl AM *et al*. Chimeric 16S rRNA sequence formation and detection in Sanger and 454-pyrosequenced PCR amplicons. *Genome Res* 2011;**21**:494–504.

Hallbeck L, Pedersen K. Autotrophic and mixotrophic growth of Gallionella ferruginea. *J Gen Microbiol* 1991;**137**:2657–61.

Hallberg KB, Johnson DB. Novel acidophiles isolated from moderately acidic mine drainage waters. *Hydrometallurgy* 2003;**71**:139–48.

Hedrich S, Schlömann M, Barrie Johnson D. The iron-oxidizing proteobacteria. *Microbiology* 2011;**157**:1551–64.

Hohmann C, Winkler E, Morin G *et al*. Anaerobic Fe(II)-oxidizing bacteria show as resistance and immobilize as during Fe(III) mineral precipitation. *Environ Sci Technol* 2010;**44**:94–101.

Hopwood MJ, Statham PJ, Skrabal SA *et al*. Dissolved iron(II) ligands in river and estuarine water. *Mar Chem* 2015;**173**:173–82.

Ionescu D, Heim C, Polerecky L *et al*. Biotic and abiotic oxidation and reduction of iron at circumneutral pH are inseparable processes under natural conditions. *Geomicrobiol J* 2015;**32**:221–30.

Islam FS, Gault AG, Boothman C *et al*. Role of metal-reducing bacteria in arsenic release from Bengal delta sediments. *Nature* 2004;**430**:68–71.

Johnson DB, Hallberg KB. The microbiology of acidic mine waters. *Res Microbiol* 2003;**154**:466–73.

Kappler A, Schink B, Newman DK. Fe(III) mineral formation and cell encrustation by the nitrate-dependent Fe(II)-oxidizer strain BoFeN1. *Geobiology* 2005;**3**:235–45.

Keim CN. Arsenic in biogenic iron minerals from a contaminated environment. *Geomicrobiol J* 2011;**28**:242–51.

Kleja DB, van Schaik JWJ, Persson I *et al*. Characterization of iron in floating surface films of some natural waters using EXAFS. *Chem Geol* 2012;**326-327**:19–26.

Klindworth A, Pruesse E, Schweer T *et al*. Evaluation of general 16S ribosomal RNA gene PCR primers for classical and next-generation sequencing-based diversity studies. *Nucleic Acids Res* 2013;**41**:e1.

Kuczynski J, Stombaugh J, Walters WA *et al*. Using QIIME to Analyze 16S rRNA gene sequences from microbial communities. *Current Protocols in Bioinformatics*. Vol Chapter 10. Hoboken, NJ: John Wiley & Sons, Inc., 2011, Unit 10.7.

Lane DJ. 16S/23S rRNA Sequencing. *Nucleic Acid Techniques in Bacterial Systematic*. New York: John Wiley. 1991.

Laufer K, Byrne JM, Glombitza C *et al*. Anaerobic microbial Fe(II) oxidation and Fe(III) reduction in coastal marine sediments controlled by organic carbon content. *Environ Microbiol* 2016a;**18**:3159–74.

Laufer K, Nordhoff M, Røy H *et al*. Coexistence of microaerophilic, nitrate-reducing, and phototrophic Fe(II) oxidizers and Fe(III) reducers in coastal marine sediment. *Appl Environ Microbiol* 2016b;**82**:1433–47.

Laufer K, Røy H, Jørgensen BB *et al*. Evidence for the existence of autotrophic nitrate-reducing Fe(II)-oxidizing bacteria in marine coastal sediment. *Appl Environ Microbiol* 2016c;**82**:6120–31.

Lewis BJ, Leighfield KG, Cox SJ, The South Wales coalfield (including the pembrokeshire coalfield): a review of mine water recovery. *Report from Wardell Armstrong for Coal Authority, Job NL02906* 2000.

Lloyd JR. Microbial reduction of metals and radionuclides. *FEMS Microbiol Rev* 2003;**27**:411–25.

Lovley DR. Microbial Fe(III) reduction in subsurface environments. *FEMS Microbiol Rev* 1997;**20**:305–13.

Lovley DR, Phillips EJP. Novel mode of microbial energy metabolism: organic carbon oxidation coupled to dissimilatory reduction of iron or manganese. *Appl Environ Microbiol* 1988;**54**:1472–80.

Lueder U, Druschel G, Emerson D *et al*. Quantitative analysis of O2 and Fe2+ profiles in gradient tubes for cultivation of microaerophilic Iron(II)-oxidizing bacteria. *FEMS Microbiol Ecol* 2018;**94**:fix177.

Melton ED, Swanner ED, Behrens S *et al*. The interplay of microbially mediated and abiotic reactions in the biogeochemical Fe cycle. *Nat Rev Microbiol* 2014;**12**:797–808.

Mesa V, Gallego JLR, González-Gil R *et al*. Bacterial, archaeal, and eukaryotic diversity across distinct microhabitats in an acid mine drainage. *Front Microbiol* 2017;**8**:1756.

Muehe EM, Kappler A. Arsenic mobility and toxicity in South and South-east Asia – a review on biogeochemistry, health and socio-economic effects, remediation and risk predictions. *Environ Chem* 2014;**11**:483.

Neubauer SC, Emerson D, Megonigal JP. Life at the energetic edge: kinetics of circumneutral iron oxidation by lithotrophic iron-oxidizing bacteria isolated from the wetland-plant rhizosphere. *Appl Environ Microbiol* 2002;**68**:3988–95.

Nevin KP, Holmes DE, Woodard TL *et al*. Geobacter bemidjiensis sp. nov. and Geobacter psychrophilus sp. nov., two novel Fe(III)-reducing subsurface isolates. *Int J Syst Evol Microbiol* 2005;**55**:1667–74.

Nordstrom DK, Alpers CN. Negative pH, efflorescent mineralogy, and consequences for environmental restoration at the Iron Mountain Superfund site, California. *Proc Natl Acad Sci USA* 1999;**96**:3455–62.

Otte JM, Harter J, Laufer K *et al*. The distribution of active iron-cycling bacteria in marine and freshwater sediments is decoupled from geochemical gradients. *Environ Microbiol* 2018;**20**:2483–99.

Overmann J. The family chlorobiaceae. *The Prokaryotes*. New York, NY: Springer, 2006, 359–78.

Park B, Dempsey BA. Heterogeneous oxidation of Fe(II) on ferric oxide at neutral pH and a low partial pressure of O2. *Environ Sci Technol* 2005;**39**:6494–500.

Parkhurst DL, Appelo CAJ, User's guide to PHREEQC (version 2)—a computer program for speciation, and inverse geochemical calculations. *Water-resources investigations report*. U.S. Geological Survey 1999.

Peine A, Tritschler A, Küsel K *et al*. Electron flow in an iron-rich acidic sediment-evidence for an acidity-driven iron cycle. *Limnol Oceanogr* 2000;**45**:1077–87.

Percent SF, Frischer ME, Vescio PA *et al*. Bacterial community structure of acid-impacted lakes: what controls diversity? *Appl Environ Microbiol* 2008;**74**:1856–68.

Pereira LB, Vicentini R, Ottoboni LMM. Changes in the bacterial community of soil from a neutral mine drainage channel. *PLoS One* 2014;**9**:e96605.

Quatrini R, Johnson DB. Microbiomes in extremely acidic environments: functionalities and interactions that allow survival and growth of prokaryotes at low pH. *Curr Opin Microbiol* 2018;**43**:139–47.

Reiche M, Lu S, Ciobotă V *et al*. Pelagic boundary conditions affect the biological formation of iron-rich particles (iron snow) and their microbial communities. *Limnol Oceanogr* 2011;**56**:1386–98.

Rhine ED, Garcia-Dominguez E, Phelps CD *et al*. Environmental microbes can speciate and cycle arsenic. *Environ Sci Technol* 2005;**39**:9569–73.

Robins NS, Davies J, Dumpleton S. Groundwater flow in the South Wales coalfield: historical data informing 3D modelling. *Q J Eng Geol Hydrogeol* 2008;**41**:477–86.

Roden EE. Microbial iron-redox cycling in subsurface environments. *Biochem Soc Trans* 2012;**40**:1249–56.

Roden EE, McBeth JM, Blöthe M *et al*. The microbial ferrous wheel in a neutral ph groundwater seep. *Front Microbiol* 2012;**3**:172.

Sapsford D, Santonastaso M, Thorn P *et al*. Conversion of coal mine drainage ochre to water treatment reagent: production, characterisation and application for P and Zn removal. *J Environ Manage* 2015;**160**:7–15.

Satola B, Wübbeler JH, Steinbüchel A. Metabolic characteristics of the species Variovorax paradoxus. *Appl Microbiol Biotechnol* 2013;**97**:541–60.

Schink B. Synergistic interactions in the microbial world. *Antonie Van Leeuwenhoek* 2002;**81**:257–61.

Schmidt C, Behrens S, Kappler A. Ecosystem functioning from a geomicrobiological perspective – a conceptual framework for biogeochemical iron cycling. *Environ Chem* 2010;**7**:399.

Shannon CE. The mathematical theory of communication. *Bell Syst Tech J* 1948;**27**:623–56.

Smedley P, Kinniburgh D. A review of the source, behaviour and distribution of arsenic in natural waters. *Appl Geochemistry* 2002;**17**:517–68.

Smedley PL, Kinniburgh DG. Arsenic in groundwater and the environment. *Essentials of Medical Geology*. Revised edn, Dodrecht, The Netherlands: Springer, 2013.

Sowers TD, Harrington JM, Polizzotto ML *et al*. Sorption of arsenic to biogenic iron (oxyhydr)oxides produced in circumneutral environments. *Geochim Cosmochim Ac* 2017;**198**:194–207.

Stams AJM, Plugge CM. Electron transfer in syntrophic communities of anaerobic bacteria and archaea. *Nat Rev Microbiol* 2009;**7**:568–77.

Stookey LL. Ferrozine-A new spectrophotometric reagent for iron. *Anal Chem* 1970;**42**:779–81.

Stumm W, Morgan JJ. *Aquatic Chemistry: Chemical Equilibria and Rates in Natural Waters*, New York: Wiley, 1993.

Sundman A, Karlsson T, Laudon H *et al*. XAS study of iron speciation in soils and waters from a boreal catchment. *Chem Geol* 2014;**364**:93–102.

Vaughan DJ, Lloyd JR. Mineral-organic-microbe interactions: environmental impacts from molecular to macroscopic scales. *Comptes Rendus Geosci* 2011;**343**:140–59.

Volant A, Bruneel O, Desoeuvre A *et al*. Diversity and spatiotemporal dynamics of bacterial communities: physicochemical and other drivers along an acid mine drainage. *FEMS Microbiol Ecol* 2014;**90**:247–63.

von der Heyden BP, Hauser EJ, Mishra B *et al*. Ubiquitous presence of Fe(II) in Aquatic colloids and its association with organic carbon. *Environ Sci Technol Lett* 2014;**1**:387–92.

Wang X-J, Yang J, Chen X-P *et al*. Phylogenetic diversity of dissimilatory ferric iron reducers in paddy soil of Hunan, South China. *J Soils Sediments* 2009;**9**:568–77.

Waters CN, Waters RA, Barclay WJ *et al*., A Lithostratigraphical Framework for the Carboniferous Successions of Southern Great Britain (Onshore). *Research report, RR/09/01*. British Geological Survey 2009.

Whiteley AS, Jenkins S, Waite I *et al*. Microbial 16S rRNA Ion Tag and community metagenome sequencing using the Ion Torrent (PGM) Platform. *J Microbiol Meth* 2012;**91**:80–8.

Widdel F, Schnell S, Heising S *et al*. Ferrous iron oxidation by anoxygenic phototrophic bacteria. *Nature* 1993;**362**:834–6.

Willems A, De Ley J, Gillis M *et al*. Comamonadaceae, a new family encompassing the acidovorans rRNA complex, including Variovorax paradoxus gen. nov., comb. nov., for Alcaligenes paradoxus (Davis 1969). *Int J Syst Bacteriol* 1991;**41**:445–50.

Wilson AD. A new method for the determination of ferrous iron in rocks and minerals. *Bull Geol Surv Gt Britain* 1955;**9**:55–8.

Wittebolle L, Marzorati M, Clement L *et al.* Initial community evenness favours functionality under selective stress. *Nature* 2009;**458**:623–6.

Wragg J, Certificate of analysis: BGS guidance material 102: Ironstone soil. *Report IR/09/006*. British Geological Survey 2009.

Yao W, Millero FJ. Oxidation of hydrogen sulfide by hydrous Fe(III) oxides in seawater. *Mar Chem* 1996;**52**:1–16.

Younger PL. The longevity of minewater pollution: a basis for decision-making. *Sci Total Environ* 1997;**194-195**: 457–66.